Vol. 128, No. 5 The American Naturalist November 1986

TWO-SEX MODELS: CHAOS, EXTINCTION, AND OTHER DYNAMIC CONSEQUENCES OF SEX

Hal Caswell and Daniel E. Weeks

Biology Department, Woods Hole Oceanographic Institution, Woods Hole, Massachusetts 02543;
Department of Biomathematics, University of California, Los Angeles, California 90024

Submitted April 17, 1985; Revised March 5, 1986; Accepted June 13, 1986

Most demographic analyses, especially the construction of life tables and estimation of rates of increase, are based on only one sex, usually the female. This practice can be justified by assuming that the life cycles of the sexes are identical or that the dynamics of the population are determined by one sex independent of the relative abundance of the other. Neither assumption is universally valid; this paper explores the dynamic consequences of relaxing them and including both sexes in demographic models of complex life cycles. First we examine some of the reasons for doubting the assumptions leading to one-sex models. Then we develop a general population-projection model incorporating both sexes and examine its dynamics.

Sexual Dimorphism in Demographic Traits

The life cycles of the sexes are certainly not always identical. Sexual dimorphism in mortality, development, and fecundity is well documented in a variety of species. In humans, male mortality almost always exceeds female mortality (e.g., Cavalli-Sforza and Bodmer 1971; Keyfitz and Flieger 1971; Wingard 1984); in the United States, the life expectancy of females at birth currently exceeds that of males by approximately 10%. Similar differences exist in countries with very different absolute levels of mortality. The dimorphism has persisted for at least several centuries (e.g., data of Bourgeois-Pichat summarized in Cavalli-Sforza and Bodmer 1971; Wingard 1984), and there is now considerable debate over how much of the difference is due to such social factors as cigarette smoking (Holden 1983; Trivers 1985).

Sexual dimorphism in mortality is also well documented in other species. Darwin (1871) compiled anecdotal evidence on horses, sheep, cattle, fowl, fish, and insects (for a recent review, see Comfort 1979). The differences often greatly exceed those observed between male and female humans. The life expectancy of female ground squirrels (*Spermophilus beldingi*) exceeds that of males by 25% (Sherman and Morton 1984). The life expectancy of the female codling moth (*Carpocapsa pomonella*) exceeds that of the male by as much as 35% (MacArthur

Am. Nat. 1986. Vol. 128, pp. 707–735.

and Baillie 1932). In the black widow spider (*Latrodectus mactans*) the female advantage is 170% (Deevey and Deevey 1945). In the copepod *Pseudocalanus*, males and females require on the order of 40 days to reach maturity, but after reaching maturity females live for more than 100 days, and males die in about 15 days (Corkett and McLaren 1978), a female advantage of 154%.

Why male mortality should be generally greater is not clear. Geiser (1924) proposed that it is caused by the expression of deleterious recessive genes carried on the sex chromosome. In species with homogametic females, such genes are expressed in males but not in females. Under this hypothesis, the dimorphism in mortality should be reversed for species in which the male is the homogametic sex (e.g., birds and the Lepidoptera). The available evidence, however, suggests that this is not the rule (MacArthur and Baillie 1932; Comfort 1979).

In at least some cases, the differences between male and female mortality probably result from the interaction of morphological or behavioral dimorphism with environmental factors. Clutton-Brock et al. (1985), for example, suggested that in mammals male mortality is higher because young males are more susceptible to food shortage; this susceptibility in turn results from higher male growth rates and nutritional requirements. Maly (1970) found sex-specific predation rates on freshwater copepods (*Diaptomus* sp.) in experiments with salamanders and fish. Salamanders fed preferentially on females; guppies fed preferentially on males. In ponds where salamanders were the major predator, the adult copepod sex ratio favored males (0.82–3.35 males per female), but in ponds where fish were the major predators the adult sex ratio favored females (0.43–0.85 males per female).

Whatever its causes, the extent of sexual dimorphism in mortality responds to environmental factors and is subject to genetic variation. Dingle (1966) found that the dimorphism in mortality increased with population density in two species of Heteroptera (in which, incidentally, male mortality was less than female mortality). MacArthur and Baillie (1932) documented a latitudinal cline in the magnitude of the female advantage in the codling moth. Pearl (1928) documented genetic variation by comparing wild-type stocks of *Drosophila melanogaster* with stocks carrying a mutant gene for vestigial wings. The vestigial mutant increased not only overall mortality but also the sex differential from a 5% female advantage in the wild type to 40% in the vestigial strain.

Significant sex differences in age at maturity are also common. At maturity females are 1.2 times the age of males in the lily *Chamaelirium luteum* (Meagher and Antonovics 1982*a*), males 2.5 times the age of females in the sperm whale, *Physeter macrocephalus* (Allen 1980), and females 2.7–3.2 times the age of males in the turtle *Pseudemys scripta* (Gibbons et al. 1981). Data compiled by Bell (1980, fig. 5) suggest that in freshwater fishes females are typically about 1.3 times the age of males at maturity, and that in mammals and birds males are typically about 1.4 times the age of females.

Finally, we note the widespread existence of sexual dimorphism in fecundity. This is more complicated than dimorphism in survival or maturity, because it depends strongly on the adult sex ratio. In particular, the variance in male and female fecundities may often differ, as demonstrated for the red deer (*Cervus elaphus*) by Clutton-Brock et al. (1982).

Sexual dimorphism in demographic traits, then, is widespread and often much more pronounced in other species than it is in humans. Recognizing that the life cycles of the sexes are not identical, one might attempt parallel but separate treatment of the sexes, constructing and analyzing separate male and female life tables. Such separate life tables, however, are generally inconsistent; that is, the rate of increase for females calculated from the female life table differs from that calculated for males from the male life table. Extrapolated, such inconsistency predicts that the relative abundance of one sex or the other will eventually decline to zero.

Dominance, Sex Ratio, and the Marriage Squeeze

The assumption of dominance by one sex is the simplest solution to the consistency problem. If the dynamics of the population are determined by one sex, then demographic calculations can be carried out using the vital rates of that sex alone. The usual assumption is "female dominance": there are always enough males to fertilize all the females.

When the assumption of dominance fails, distortions of the sex ratio result in a "marriage squeeze" (Schoen 1983), in which marriage, and by implication reproduction, is limited by the availability of the scarcer sex. Marriage squeezes are well known, even in large human populations, where the overall sex ratio never deviates very far from unity. Patterns of preference for age and educational background (Goldman et al. 1984) in a mate can result in marked marriage squeezes (e.g., Long Island, New York, with an estimated 49.2 eligible men per 100 women; The Economist 1985).

That fluctuations in the sex ratio may affect reproduction in nonhuman populations has been demonstrated in the laboratory (Wade 1984), and the use of such effects has been proposed as a component of biological-control programs (Hamilton 1967; Robinson 1983). Some haplodiploid species colonizing ephemeral resources may use their ability to bias the sex ratio of their offspring by controlling fertilization to maximize their initial population growth rate after colonization (Gould 1983, chap. 4). Seed production in some plants is known to be limited by pollen availability (see review in Willson and Burley 1983), which is in effect a shortage of males.

All other things being equal, marriage squeezes are most likely when the adult sex ratio differs substantially from unity. The sex ratio in human populations seldom does so; typical values in the compilation of Keyfitz and Flieger (1971) differ by only a few percent from a male:female ratio of unity. However, adult sex ratios in other species vary more widely. Willson (1983), for example, tabulated sex ratios for angiosperms ranging from less than 0.1 to 191 males per female; ratios as low as 0.5 and as high as 3 are common. Sex ratios for aquatic animals (Altman and Dittmer 1962; Maly 1970) range from less than 0.1 to over 10, for mammals from 0.25 to 2.7 (Altman and Dittmer 1962; Nevo 1979), and for birds from 0.35 to 3.3 (Altman and Dittmer 1962).

Sex ratios are not constant within species. Maufette and Jobin (1985) found sex ratios from 0.46 to 1.99 in a sample of 13 local populations of gypsy moth (*Lymantria dispar*). Alstad and Edmunds (1983) found sex ratios in local populations of the black pineleaf scale (*Nuculaspis californica*) from 0.005 to 0.320 in a sample of 18 trees measured over 3 yr. Tande and Gronvik (1983) documented a seasonal sex-ratio cycle in the marine copepod *Metridia longa*: males are common in the winter ($\approx$20 males per female) and rare in the summer ($\approx$0 males per female). Marshall and Orr (1955, p. 29), speaking of the copepod *Calanus finmarchicus*, stated, "In plankton catches females usually out-number males greatly and although this is partly because of the shorter life of the males and partly because their maximum number occurs earlier in the breeding cycle than that of the females, it still remains a problem how all the females, especially those moulting late, can be fertilized." (Note that the collection and interpretation of such sex-ratio data can be complicated because demographic dimorphism is often associated with ecological and behavioral differences that make it hard to sample both sexes in comparable fashion; Ehrlich et al. 1984).

Mating squeezes resulting from fluctuating sex ratios may be more important, and will certainly be more complex, in species that exhibit more-varied patterns of sexuality, such as sex reversal (Charnov 1982; Policansky 1982) or multiple mating strategies. In Atlantic salmon (*Salmo salar*), for instance, some males mature precociously without going to sea. These precocious males cannot mate with adult females, but sneak fertilizations from pairs of mating adults. Their reproductive output thus depends in a potentially complicated way on the relative frequencies of females, precocious males, and adult males in the population. The frequency of precocious maturation varies in both space and time (Jones 1959; Caswell et al., MS), and its adaptive significance depends on the relative fitnesses of each of the three types (cf. Caswell et al. 1984; Gross 1984). Similar alternative male strategies are well known in other species (e.g., Gross 1984). Such complications reach a baroque extreme in the basidiomycete fungi, populations of which may contain hundreds or even thousands of mating types (Raper 1966).

TWO-SEX MODELS

If the life cycles of the sexes differ and the assumption of dominance fails, both sexes must be incorporated into demographic models. The resulting models are necessarily nonlinear, because only in a nonlinear model can reproduction depend on the relative abundance of males and females.

Human demographers have addressed the problem since the 1940s (see reviews in Keyfitz 1972; Pollard 1977). However, they have devoted relatively little attention to the dynamics of two-sex models for structured populations. Much of the human demographic literature focuses on the consistency problem (how to make the estimates of r based on male and female life tables agree; see the review in Das Gupta 1978) and ignores dynamics. The studies that have considered dynamics in any detail (e.g., Keyfitz 1968; Pollard 1973; Samuelson 1976; Yellin and Samuelson 1977; Luppova and Frisman 1983; Schoen 1984) have focused on models without age structure.

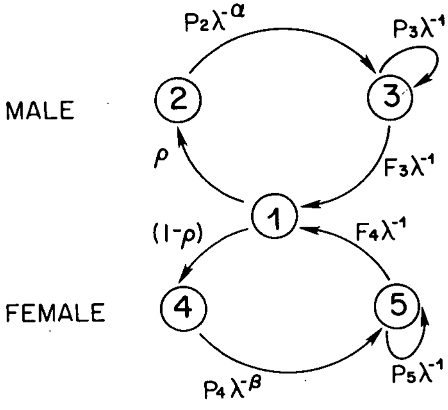

FIG. 1.—A life-cycle graph for a simple two-sex population model. Stage 1 represents "zygotes," which are produced jointly by adult males (n_3) and females (n_5) but which have not yet been assigned a sex. The P_i are survival probabilities; F_i, the per capita fecundities; ρ, the primary sex ratio. The negative exponent on λ denotes the time required for the transition; thus, α and β are, respectively, the male and female ages at maturity.

In this paper we examine three simple two-sex models for age-structured populations. Our approach, and some of our results, apply to other frequency-dependent interactions in more-complex life cycles. We consider several alternative descriptions of the interaction between the sexes, the resulting nature of the equilibrium population structure (especially the adult sex ratio), the stability of that structure, and the dynamic consequences of instabilities.

MODEL I: HOMOGENEOUS MODELS AND BASIC STABILITY RESULTS

The Life-Cycle Graph

We consider first a simple model based on the life-cycle graph in figure 1 (for a discussion of this representation of the life cycle, see Caswell 1982). Males are shown in the upper half of the graph, females in the lower half. Adults have age-independent survival probabilities of P_3 and P_5. Males require α time units and females β time units to reach maturity. Adult males and females produce sexually undifferentiated "zygotes" (n_1). The primary sex ratio (the proportion of males) is given by ρ; this fraction of the zygotes is assigned to n_2 and the complement to n_4. This description of reproduction is convenient, but our approach does not depend on it; we could present an equivalent graph showing the direct production of male and female offspring by males and females.

If the life cycle were time-invariant, the graph could be analyzed using z-transform methods (Hubbell and Werner 1979; Caswell 1982). In such analyses λ denotes the population growth rate, and the negative exponent on λ gives the time required for the transition. In a two-sex model, however, the life-cycle graph will vary with time unless the population is at an equilibrium age-sex composition. We include the exponents in the graph anyway, although they will be of formal use only at equilibrium.

In figure 1 the transition from the zygote stage (n_1) to n_2 or n_4 is assumed to require one unit of time; this could be modified. Cases in which the sexes cannot be distinguished at birth, or in which sex is determined environmentally some time after birth (Adams et al. 1985), may be conveniently treated by increasing the lag in the transitions from n_1 to n_2 and from n_1 to n_4.

The per capita male and female fecundities F_3 and F_5, respectively, are nonlinear functions of the relative abundance of males and females, described in detail below.

The dynamics of this population can be described by a nonlinear projection matrix, the nature of which depends on the structure of the life-cycle graph (see Caswell 1982). For example, supposing that $\alpha = 2$ and $\beta = 3$, the matrix corresponding to figure 1 is

$$\mathbf{A} = \begin{pmatrix} 0 & 0 & 0 & F_3 & 0 & 0 & 0 & F_5 \\ \rho & 0 & 0 & 0 & 0 & 0 & 0 & 0 \\ 0 & P_2 & 0 & 0 & 0 & 0 & 0 & 0 \\ 0 & 0 & 1 & P_3 & 0 & 0 & 0 & 0 \\ 1-\rho & 0 & 0 & 0 & 0 & 0 & 0 & 0 \\ 0 & 0 & 0 & 0 & P_4 & 0 & 0 & 0 \\ 0 & 0 & 0 & 0 & 0 & 1 & 0 & 0 \\ 0 & 0 & 0 & 0 & 0 & 0 & 1 & P_5 \end{pmatrix}.$$

The dynamics of the population are given by

$$\mathbf{n}(t + 1) = \mathbf{A}_n \mathbf{n}(t). \tag{1}$$

The subscript indicates that $\mathbf{A}$ depends on $\mathbf{n}$; it will be suppressed where no ambiguity results. Equation (1) can also be written as a nonlinear map:

$$\mathbf{n}(t + 1) = \pi[\mathbf{n}(t)]. \tag{2}$$

The nonnegativity of the matrix $\mathbf{A}$ (i.e., all $a_{ij} \geq 0$) implies that the function $\pi(\ )$ maps the set of all nonnegative vectors into itself.

The Birth and Fecundity Functions

The per capita fecundities, F_i, in figure 1 are actually the functions $F_i(\mathbf{n})$ of the current population structure; they summarize the demographic interactions between the sexes. The fecundity function is most easily derived from the birth function $B(\mathbf{n})$ (sometimes known in human demography as marriage function). $B(\mathbf{n})$ gives the number of births produced by the population $\mathbf{n}$. Biological considerations (cf. Frederickson 1971; Das Gupta 1972; McFarland 1972; Yellin and Samuelson 1974) suggest that $B(\mathbf{n})$ should satisfy certain criteria. For convenience, suppose that, as in figure 1, there is only one class of males (n_{m}) and one of females (n_{f}).

1. $B(n_{\mathrm{m}}, n_{\mathrm{f}})$ should be well defined and nonnegative for all nonnegative values of n_{m} and n_{f}.

2. $B(n_{\mathrm{m}}, n_{\mathrm{f}})$ should be a first-degree homogeneous function of its arguments;

that is, $B(cn_{\mathrm{m}}, cn_{\mathrm{f}}) = cB(n_{\mathrm{m}}, n_{\mathrm{f}})$ for any nonnegative c. As will become clear when we derive per capita fecundity functions, this requirement ensures that reproduction depends on the relative, rather than the absolute, abundance of the sexes.

3. $B(0, n_{\mathrm{f}}) = B(n_{\mathrm{m}}, 0) = 0$. No births should occur in the absence of either males or females.

4. $B(n_{\mathrm{m}}, n_{\mathrm{f}})$ should be a non-decreasing function of the n_{m} and n_{f}.

5. It seems plausible in many circumstances that, given a fixed number of one sex, births should eventually grow at a decreasing rate as the number of the other sex increases; that is, $\partial^2 B/\partial n_{\mathrm{m}}^2 < 0$ for sufficiently large n_{m}, and similarly for n_{f}. It may even be reasonable for $B(\ )$ to approach a constant limit as n_{m} or n_{f} approaches ∞.

Human demographers have examined a number of birth or marriage functions, setting $B(n_{\mathrm{m}}, n_{\mathrm{f}})$ proportional to

n_{f}	(female dominant)	$(n_{\mathrm{m}} n_{\mathrm{f}})^{1/2}$	(geometric mean)
n_{m}	(male dominant)	$\dfrac{2n_{\mathrm{m}} n_{\mathrm{f}}}{n_{\mathrm{m}} + n_{\mathrm{f}}}$	(harmonic mean)
$an_{\mathrm{m}} + (1 - a)n_{\mathrm{f}}$	(weighted mean)	$\min(n_{\mathrm{m}}, n_{\mathrm{f}})$	(minimum)

Each of these functions has been rejected by human demographers (McFarland 1972) for one reason or another, but the harmonic mean is regarded as the least flawed. Attempts to distinguish between them based on observed marriage rates have been frustrated by the limited range of sex ratios occurring in human populations (Keyfitz 1972). We know of no attempts to distinguish them experimentally by using other species in the laboratory.

The per capita fecundity functions, $F_i(\mathbf{n})$, are derived from the birth function. By definition,

$$B(n_{\mathrm{m}}, n_{\mathrm{f}}) = n_{\mathrm{m}} F_{\mathrm{m}} + n_{\mathrm{f}} F_{\mathrm{f}}. \tag{3}$$

Assuming that each zygote has exactly one parent of each sex, such that $n_{\mathrm{m}} F_{\mathrm{m}} = n_{\mathrm{f}} F_{\mathrm{f}}$ (and thereby excluding such considerations as haplodiploidy), equation (3) can be rewritten as

$$F_{\mathrm{m}} = B(n_{\mathrm{m}}, n_{\mathrm{f}})/2n_{\mathrm{m}} \tag{4a}$$

and

$$F_{\mathrm{f}} = B(n_{\mathrm{m}}, n_{\mathrm{f}})/2n_{\mathrm{f}}. \tag{4b}$$

For the harmonic-mean birth function, the female fecundity function is

$$F_{\mathrm{f}} = n_{\mathrm{m}}/(n_{\mathrm{m}} + n_{\mathrm{f}}), \tag{5}$$

with a similar expression for males. The per capita fecundity of a female increases hyperbolically with the abundance of males (for fixed n_{f}), and decreases with the abundance of females (for fixed n_{m}).

Clutch size.—The birth functions defined above give, in effect, the number of matings as a mean of the abundance of the two sexes. If females produce multiple offspring, the number of matings is multiplied by the average clutch size (k) to give the number of births.

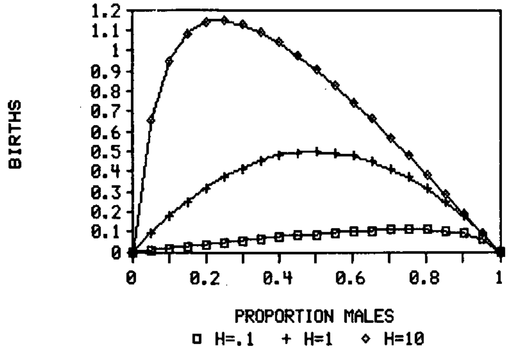

FIG. 2.—The harmonic-mean birth function $B(n_{\mathrm{m}}, n_{\mathrm{f}})$ (eq. 6), as a function of the proportion of one sex in the population and the harem size h.

Harem size.—Equating the number of matings to a mean of n_{m} and n_{f} assumes monogamous mating. If males maintain harems of average size h ($h > 1$ corresponds to polygyny, $h < 1$ to polyandry; see Rosen 1983), $B(\ )$ should be written as the harmonic mean of the number of males and the number of harems, $H = n_{\mathrm{f}}h^{-1}$. The relevant clutch size is now the number of offspring produced per harem, which equals kh. Thus, the harmonic-mean birth function becomes

$$B(n_{\mathrm{m}}, n_{\mathrm{f}}) = 2kn_{\mathrm{m}}n_{\mathrm{f}}/(n_{\mathrm{m}} + n_{\mathrm{f}}h^{-1}), \tag{6}$$

and the corresponding fecundity function is

$$F_{\mathrm{f}} = kn_{\mathrm{m}}/(n_{\mathrm{m}} + n_{\mathrm{f}}h^{-1}). \tag{7}$$

When harem size $h = 1$, births are maximized when males and females are equally abundant. If $h > 1$, however, B is maximized when females exceed males; to be precise, B is maximized when $n_{\mathrm{f}} = n_{\mathrm{m}}\sqrt{h}$ (fig. 2). This adult sex ratio maximizes population growth rate, although it is not evolutionarily stable (Fisher 1958). Larger harem sizes also make female fecundity less dependent on the sex ratio (figs. 3*a*,*b*); in the limit as $h \to \infty$, births become female-dominant. Male fecundity increases with harem size, and becomes more sensitive to the adult sex ratio (figs. 3*c*,*d*).

Frequency and Density Dependence

We can now distinguish frequency and density dependence. The nonlinear map (eq. 2) is frequency-dependent if $\pi(\mathbf{n})$ is homogeneous of degree 1. The elements a_{ij} of the corresponding matrix model (1) are then homogeneous of degree zero in their arguments, that is, $a_{ij}(c\mathbf{n}) = a_{ij}(\mathbf{n})$ for any $c > 0$. The demographic properties of such a population depend only on the relative magnitude of the n_i, and not at all on their absolute magnitude. A matrix not satisfying this condition has at least some degree of density dependence. Requiring $B(\mathbf{n})$ to be homogeneous of degree one guarantees that the $F_i(\mathbf{n})$ are homogeneous of degree zero. Thus, two-sex models based on the harmonic mean (including variable harem size) are strictly frequency-dependent.

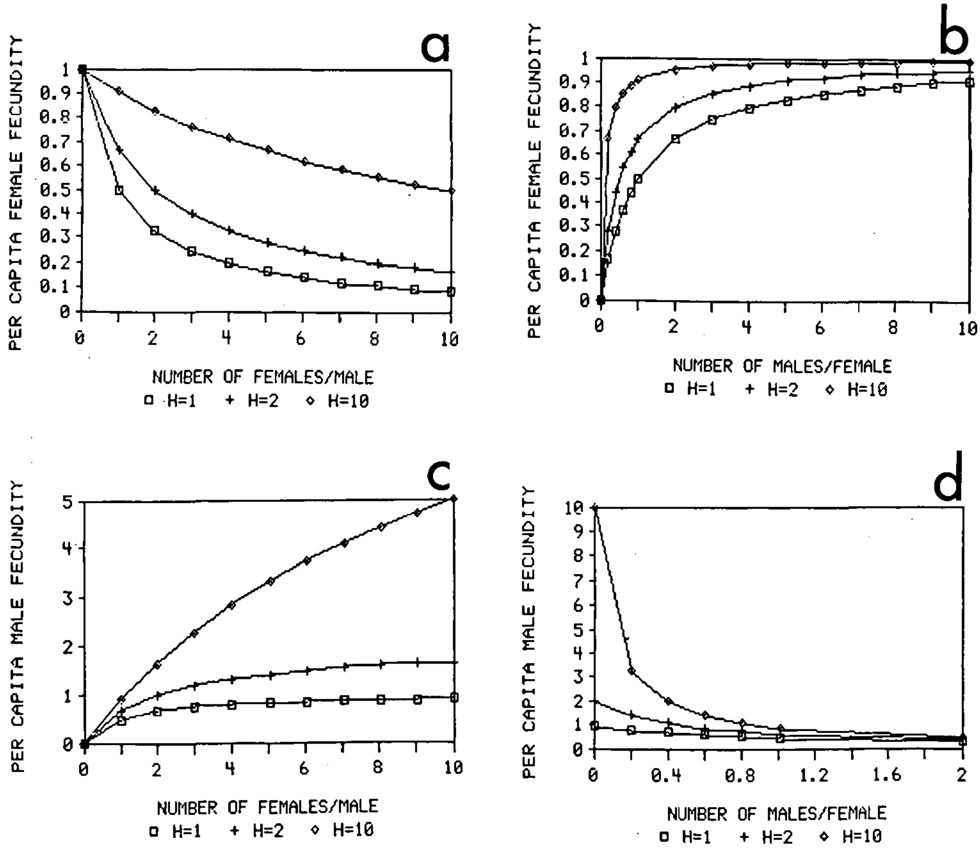

FIG. 3.—Per capita male and female fecundities derived from the harmonic-mean birth function with variable harem size (eq. 7): *a*, female fecundity as a function of the number of females per male; *b*, female fecundity as a function of males per female; *c*, male fecundity as a function of females per male; *d*, male fecundity as a function of males per female.

A biologically relevant two-sex fecundity function that is not strictly frequency-dependent is the sigmoid function

$$F_m = kn_f^\epsilon/(n_m + n_f^\epsilon) \tag{8}$$

for $\epsilon > 1$ (fig. 4). Such a function might be generated by social facilitation of mating or by the process of searching for mates at low densities. Its dynamic consequences are discussed below.

The Equilibrium Adult Sex Ratio

An equilibrium population structure, which automatically implies an equilibrium sex ratio, is given by any vector $\mathbf{w}$ satisfying

$$\mathbf{A}\mathbf{w} = \lambda\mathbf{w} \tag{9}$$

for some constant λ, which gives the growth rate of the population at equilibrium.

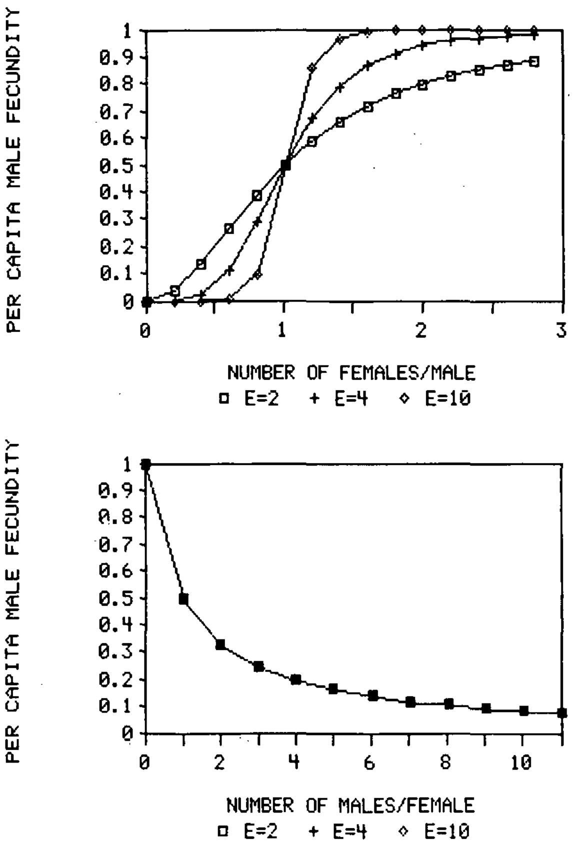

FIG. 4.—Male per capita fecundity calculated using the sigmoid fecundity function (eq. 8), for one male and varying numbers of females (*top*) and for one female and varying numbers of males (*bottom*). As the parameter ϵ (denoted by E in the graph captions) increases, male fecundity increases more sharply as the number of females increases. The value of ϵ has no effect on the rate of decline of male fecundity with the relative abundance of males.

The zero vector is always a (trivial) solution to equation (9). The existence of a nontrivial solution is guaranteed if the matrix **A** is continuous and frequency-dependent, and if **A** does not map any nonzero vector directly to zero (Nussbaum 1986). To see this, define $\mathbf{x} = \mathbf{n}/\Sigma n_i$ as the vector of proportions in the different stages. Then define the map $\phi(\mathbf{x})$ by

$$\mathbf{x}(t+1) = \pi[\mathbf{x}(t)]/\Sigma x_i(t) = \phi[\mathbf{x}(t)].$$

Since $\phi(\ )$ is a continuous map from a closed, bounded set into itself, Brouwer's fixed-point theorem guarantees the existence of a fixed point $\hat{\mathbf{x}}$ satisfying $\hat{\mathbf{x}} = \phi(\hat{\mathbf{x}})$. The homogeneity of $\pi(\ )$ implies that any vector **w** proportional to $\hat{\mathbf{x}}$ satisfies equation (9), and represents an equilibrium population structure.

Any life-cycle graph with a self-loop in the last stage within each sex (e.g., figs. 1, 6) satisfies this condition, which is certainly more stringent than necessary.

If an equilibrium population structure **w** exists, its elements can be written down directly from the life-cycle graph (Caswell 1982). Since **A** is homogeneous of degree zero, its variable elements become constant along the trajectory $\mathbf{n}(t+1) = \lambda\mathbf{n}(t)$, equation (9) reduces to a standard eigenvalue problem, and **w** is the right eigenvector of **A**. Using the eigenvector formulas in Caswell (1982), the population structure corresponding to the life cycle of figure 1 is

$$\begin{aligned} w_1 &= 1 & w_4 &= (1-\rho)\lambda^{-1} \\ w_2 &= \rho\lambda^{-1} & w_5 &= (1-\rho)[P_4\lambda^{-\beta}/(\lambda - P_5)]. \\ w_3 &= \rho[P_2\lambda^{-\alpha}/(\lambda - P_3)] \end{aligned} \tag{10}$$

The growth rate at equilibrium (λ) appears in **w** as a parameter; it is obtained from the characteristic equation

$$1 = \rho\frac{P_2F_3\lambda^{-(\alpha+1)}}{\lambda - P_3} + (1-\rho)\frac{P_4F_5\lambda^{-(\beta+1)}}{\lambda - P_5}. \tag{11}$$

Since F_3 and F_5 are at equilibrium themselves functions of **w**, equations (10) and (11) must be solved simultaneously to obtain λ and **w**.

The equilibrium adult sex ratio $R = n_3/n_5$ is given by

$$R = \left(\frac{\rho}{1-\rho}\right)\left(\frac{P_2}{P_4}\right)\left[\frac{\lambda^{\beta-\alpha}(\lambda - P_5)}{\lambda - P_3}\right], \tag{12}$$

from which we see that the equilibrium sex ratio favors the sex with the higher juvenile survival, the shorter maturation time, and the higher adult survival. The maturation-time effect is amplified by population growth rate: if $\lambda = 1$, it disappears; if $\lambda < 1$, it is reversed. The nonlinearity introduced by the fecundity functions affects R only through the value of λ. Meagher (1981, 1982; Meagher and Antonovics 1982*a*,*b*) derived a similar formula from a different projection matrix, the elements of which are themselves functions of λ.

The reproductive values of each stage can also be written down directly from figure 1 (Caswell 1982):

$$\begin{aligned} v_1 &= 1 & v_4 &= P_4F_5\lambda^{-\beta}/(\lambda - P_5) \\ v_2 &= P_2F_3\lambda^{-\alpha}/(\lambda - P_3) & v_5 &= F_5/(\lambda - P_5). \\ v_3 &= F_3/(\lambda - P_3) \end{aligned} \tag{13}$$

The nonlinear fecundity functions appear explicitly in **v**, so that reproductive value depends directly on population composition through the F_i, as well as indirectly through λ. The reproductive-value formulas can be used for sensitivity analysis of the population growth rate at equilibrium.

Stability of the Equilibrium Sex Ratio

When will a population with some other composition converge to an equilibrium structure **w**? A number of two-sex models without age structure have been shown to be stable (e.g., Keyfitz 1968; Pollard 1973; Samuelson 1976; Yellin and Samuelson 1977; Schoen 1984), with the exception of some declining populations (Yellin and Samuelson 1977). Similar claims of stability have been made (Das Gupta 1972; Mitra 1978) for age-classified models, which at equilibrium reduce to the classical renewal equation of the one-sex case. These results, however, rely on the constancy of fecundities at equilibrium to eliminate the effects of the nonlinearity in the birth function. In fact, the characteristic equation of any frequency-dependent model reduces at equilibrium to the same form as that of a one-sex model, but this says nothing about convergence from initial conditions that do not lie on the equilibrium solution.

Instability of the equilibrium population structure, if it occurs, might be followed by bifurcations, periodic oscillations, and chaotic behavior. This is known to occur in density-dependent demographic models (e.g., Guckenheimer et al. 1977; Levin and Goodyear 1980). This would represent a new class of population instabilities, with presently unknown consequences.

In this section, we present a theorem that gives sufficient conditions for the local stability of the equilibrium population structure. We have purposely phrased it so that it is not restricted to the life cycle shown in figure 1. In fact, it applies to a wide class of frequency-dependent population processes.

We assume that the elements a_{ij} of the matrix **A** are derived from generalized means of the elements of n. Consider a set of variables x_i and a set of nonnegative weights p_i satisfying $\Sigma p_i = 1$. Following Hardy et al. (1952), we define a generalized mean of the x_i as

$$M_r(x) = \left(\sum_i p_i x_i^r\right)^{1/r}. \tag{14}$$

When $r = 1$, M_r is the arithmetic mean; $r = 0$ gives the geometric mean, and $r = -1$ the harmonic mean. The $\lim_{r\to\infty} M_r$ is the maximum and $\lim_{r\to-\infty} M_r$ the minimum of the x_i. This formulation is thus general enough to accommodate all of the commonly used birth functions. Indeed, birth functions based on any mean with $r \leq 0$ satisfy the important condition that the absence of one sex leads to no births.

We assume that each element of **A** is derived from a generalized mean of some set comprising stage abundances or linear combinations of those abundances. In equation (6), for example, the fecundity function was derived from the harmonic mean of n_{m} and n_{f}/h. Define this set $X = \{x\}$, where each $x \in X$ is a nonnegative linear combination of the n_i. Then, we assume that every a_{ij} can be written

$$a_{ij} = k_{ij} M_{ij}(X_{ij})/n_j, \tag{15}$$

where k_{ij} is an arbitrary constant and M_{ij} is some mean. The exponent r in the mean, in general, differs from one element of **A** to another, as does the set of elements over which the mean is taken. Note that a constant a_{ij} follows from letting $X = \{n_j\}$, in which case $a_{ij} = k_{ij}$.

We also assume that n_j appears in at least one of the elements of X_{ij}. That is, the mean involved in calculating the transition from n_j to n_i depends on the abundance of the "source" stage. This assumption is stronger than necessary, as will be discussed below.

Equation (15) should be compared to the calculation of the fecundity functions from the birth function (4). The coefficient a_{ij} gives the per capita production of stage i by stage j individuals. Equation (15) asserts that this is proportional to a mean of the abundances of some subset of the population, weighted by terms representing, for example, harem size and then divided by the abundance of stage j.

Since any mean is homogeneous of degree one, the a_{ij} defined by equation (15) are homogeneous of degree zero, and the system is frequency-dependent. However, we have made no assumptions about where in the life cycle the nonlinear terms appear, what subsets of the population influence them, or what type of means are involved in their calculation. Our main result is given in the following theorem.

Theorem 1.—If the matrix $\mathbf{A}$ is defined by equation (15) and is primitive when evaluated along $\mathbf{n} = \mathbf{w}$, then any initial population near the stable population structure $\mathbf{w}$ converges to $\mathbf{w}$; thus, the sex ratio is locally asymptotically stable.

Proof.—The proof relies on a generalization of the usual local stability analysis of nonlinear matrix models (e.g., Beddington 1974) and is given in Appendix A. Nussbaum (1986) proved some global stability results for a related class of nonlinear maps.

Figure 5 shows some examples of convergence to the stable sex ratio. The rate of convergence is inversely related to the extent of sexual dimorphism in demographic traits. If male and female survival or development differ greatly, convergence may be slow and the transient oscillations large. The assumption that natural populations are close to their equilibrium sex ratio may be as questionable as the assumption that they are near the stable age distribution.

As general as the assumptions of theorem 1 may be, one undeniably important factor is *excluded* from equation (15), inter-stage mate competition. According to (15), a_{ij} correlates negatively with the abundance of only one stage (n_j). It correlates positively with the abundance of any of the other stages that appear in X_{ij}. Thus, the per capita production of stage i by stage j is reduced by competition *within* stage j, but not by competition among different stages. Competition between males or females of different ages for access to mates is excluded. Even human demographers have criticized birth functions that leave out competition (McFarland 1972; Parlett 1972; Pollard 1977), because the rate of marriage between males and females of given ages depends not only on the relative abundance of those age groups, but also on the abundance of other age groups. The phenomenon is probably even more important in many nonhuman species. As we will show, including it dramatically alters the stability properties of the model.

MODEL 2: INTER-STAGE MATE COMPETITION

We turn now to the effects of inter-stage competition for mates. We modify the life cycle of figure 1 to include two reproductive age classes of males and females (fig. 6). The fecundity functions $F_i(\ )$ must now incorporate the contributions of all possible combinations of male and female stages. Following Frederickson (1971), Das Gupta (1972, 1978), Parlett (1972), Schoen (1981), and Pollak (1986), we write the births, $B(\mathbf{n})$, as a sum of the contributions of matings classified by male and female age:

$$B(\mathbf{n}) = \sum_i \sum_j B_{ij}(\mathbf{n}), \qquad (16)$$

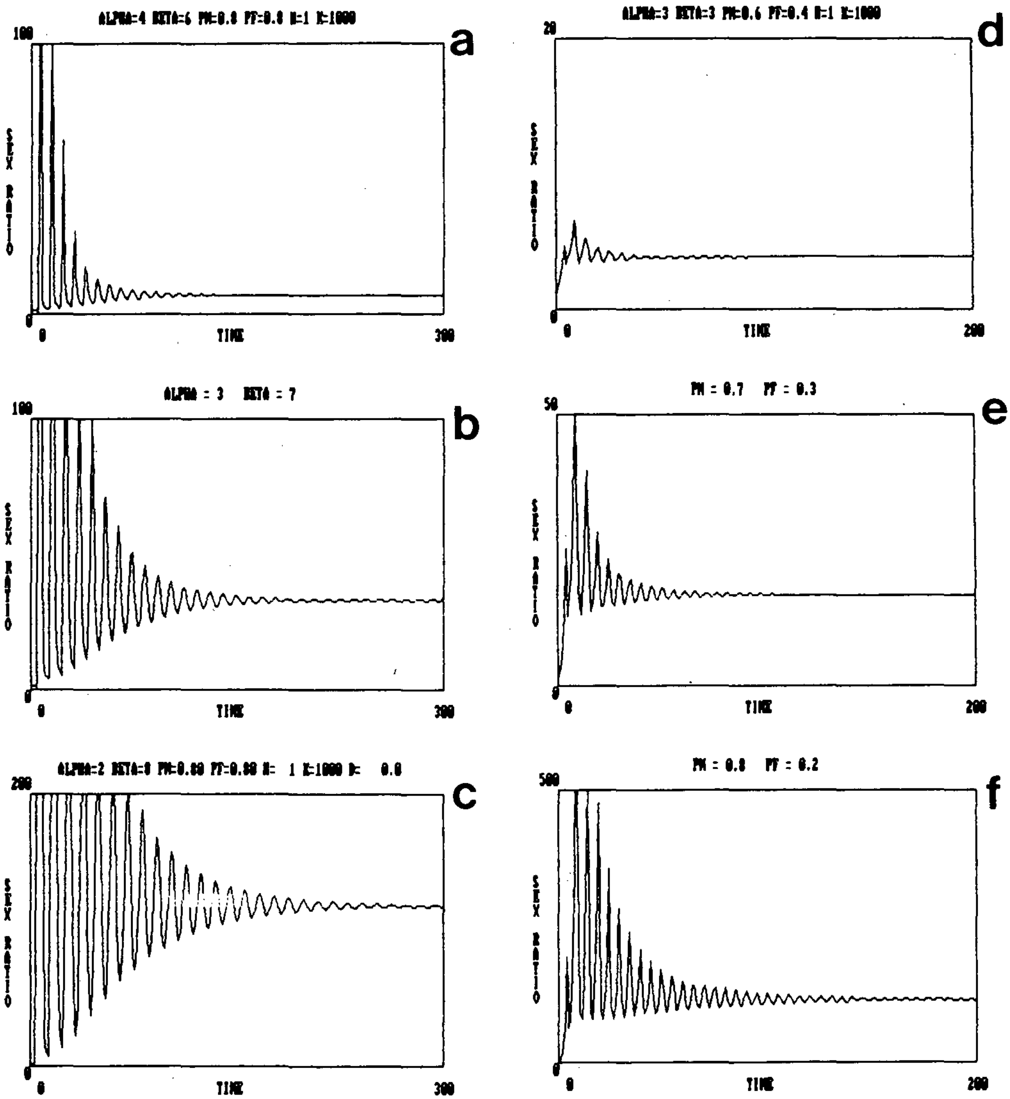

FIG. 5.—Transient dynamics of the sex ratio (males per female) as a function of the difference between male and female survival and development. *a–c*, The average development time is fixed at 5, and the difference between male and female development increases from 2 ($\alpha = 4$, $\beta = 6$) to 4 ($\alpha = 3$, $\beta = 7$) to 6 ($\alpha = 2$, $\beta = 8$). *d–f*, The average survival probability is fixed at 0.5, and the difference increased from 0.2 ($P_m = 0.6$, $P_f = 0.4$) to 0.4 ($P_m = 0.7$, $P_f = 0.3$) to 0.6 ($P_m = 0.8$, $P_f = 0.2$). Note the changes in vertical scale. Simulation details: life cycle as in figure 1; harmonic-mean birth function; harem size $h = 1$; clutch size $k = 100$. Age-independent survival rates P_m and P_f were assigned to males and females; thus, $P_3 = P_m$, $P_2 = P_m^{\alpha}$, $P_5 = P_f$, and $P_4 = P_f^{\beta}$. Initial conditions: all age groups are equally abundant.

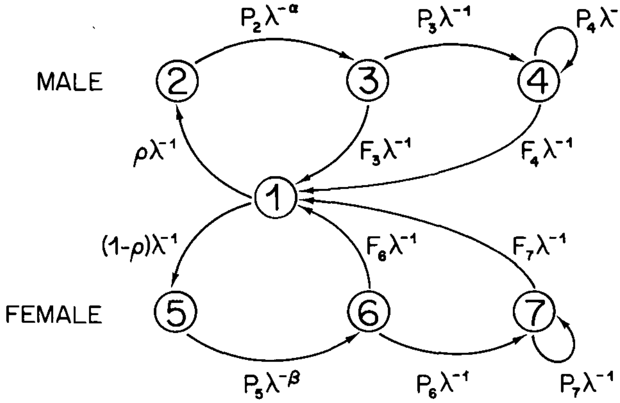

FIG. 6.—A life-cycle graph incorporating two reproductive classes of both males and females. The parameters are obvious extensions of those in figure 1.

where i is the stage of the father and j the stage of the mother. The per capita fecundity of a male of age x is then given by

$$F_x = \frac{1}{n_x} \sum_j B_{xj}(\mathbf{n}), \tag{17}$$

and that of a female of age y by

$$F_y = \frac{1}{n_y} \sum_i B_{iy}(\mathbf{n}). \tag{18}$$

The mere addition of extra age classes does not change the stability properties of the model. If the birth functions in the summations of equations (17) and (18) have the form of equation (15), the equilibrium sex ratio is still locally stable (see note 2 to Appendix A).

However, we can add inter-stage competition by maintaining the assumptions of theorem 1, except that we now replace equation (15) by

$$a_{ij} = \Sigma_h M_{ijh}(X_{ijh})/(n_j + C_{ij}). \tag{19}$$

The index h ranges over some set that produces a sum of birth-contribution terms like those in equation (16). C_{ij} is a competition term. Define c_k as a measure of the competitive effect of n_k on n_j. Then

$$C_{ij} = \sum_k c_k n_k. \tag{20}$$

Under these assumptions, **A** is still frequency-dependent. The difference between equations (19) and (15) is simply that per capita fecundity of stage j is now reduced not only by its own abundance, but also by the abundance of all the other stages appearing in the competition term (20). This is a purely phenomenological description of the effects of inter-stage competition, with some analogies to competitive inhibition in models of enzyme kinetics. Pollard (1977) proposed a

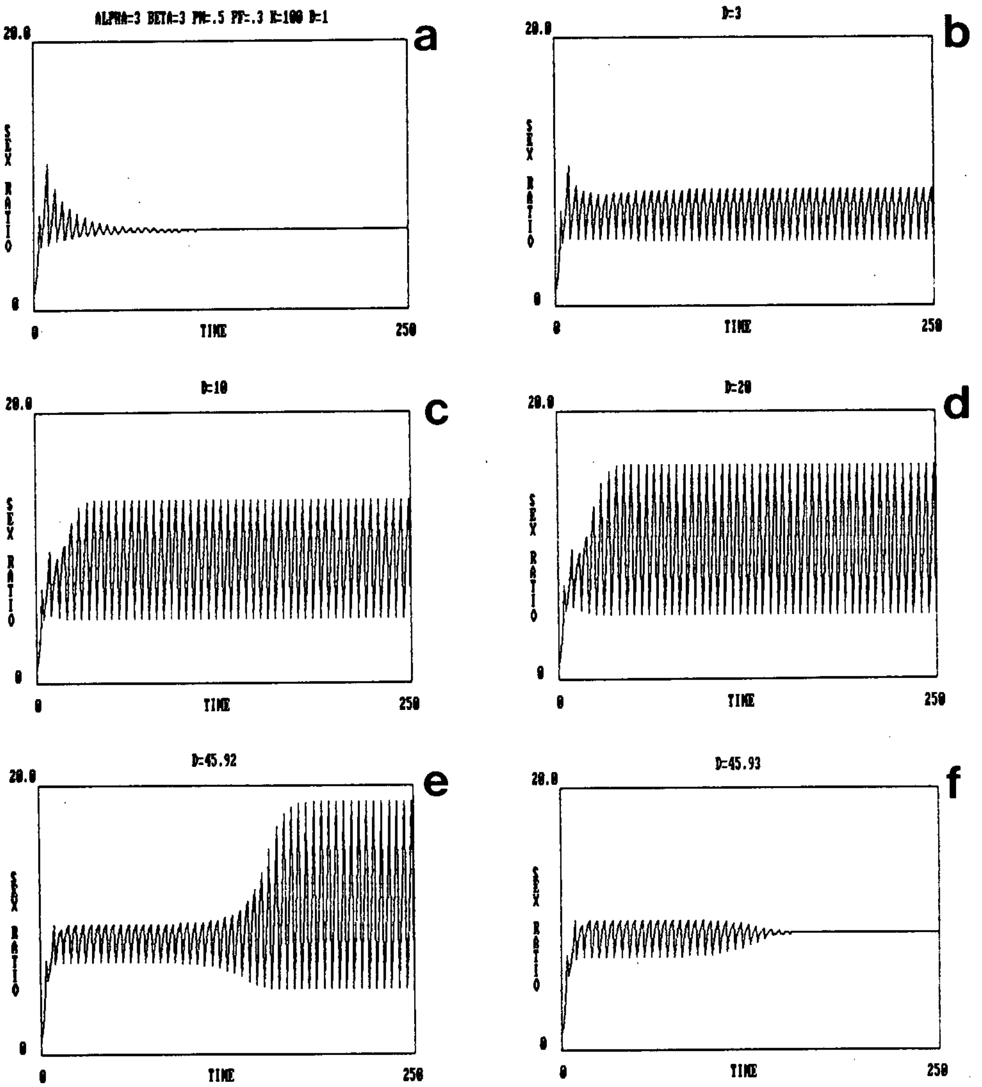

FIG. 7.—An example of bifurcation of the stable sex ratio as inter-stage competition (D) increases when male and female development times are identical. Simulation details: the life-cycle graph is as in figure 6, with fecundity functions given in equations (21). $\alpha = \beta = 3$, $P_m = 0.5$, $P_f = 0.3$, and $k_{36} = k_{37} = k_{46} = k_{47} = 100$ throughout. Initial conditions: all age groups are equally abundant. The sex ratio is defined as $(n_3 + n_4)/(n_6 + n_7)$.

special case of equation (19) as a model for marriage competition without analyzing its dynamics.

The stability proof (Appendix A) fails in the presence of inter-stage mate competition (Appendix B). In the next section, we present numerical results showing that competition can actually destabilize the equilibrium population structure, and examine some of the resulting bifurcation patterns.

Numerical Results: Competition and Instability

The following numerical results use the life cycle in figure 6, with fecundities given by

$$\begin{aligned} F_3 &= [k_{36}M(n_3, n_6) + k_{37}M(n_3, n_7)]/(n_3 + Dn_4) \\ F_4 &= [k_{46}M(n_4, n_6) + k_{47}M(n_4, n_7)]/(n_4 + Dn_3) \\ F_6 &= [k_{36}M(n_3, n_6) + k_{46}M(n_4, n_6)]/(n_6 + Dn_7) \\ F_7 &= [k_{37}M(n_3, n_7) + k_{47}M(n_4, n_7)]/(n_7 + Dn_6), \end{aligned} \tag{21}$$

where the clutch size produced by a mating between a male of stage i and a female of stage j is $2k_{ij}$ and $M(\,)$ denotes the harmonic mean with harem size, h, equal to 1. D is a coefficient that gives the intensity of inter-stage mate competition; it measures the extent to which the per capita fecundity of one stage is reduced by the presence of the other stage of the same sex. For simplicity, this competition is assumed to be symmetrical; this will certainly not be true in general.

For purposes of these simulations, males and females are assigned age-independent survival probabilities (P_m and P_f). In terms of these probabilities, the coefficients in figure 6 are $P_3 = P_4 = P_m$, $P_2 = P_m^\alpha$, $P_6 = P_7 = P_f$, and $P_5 = P_f^\beta$. All simulations were carried out on an IBM PC with an Intel 8087 numeric coprocessor in 64-bit precision.

When $D = 0$, theorem 1 applies and the equilibrium population structure is stable. Figure 7 shows the results of increasing D when the male and female development times (α and β, respectively) are identical; the adult sex ratio $(n_3 + n_4)/(n_6 + n_7)$ is plotted.

Between $D = 1.8$ and $D = 2.5$ the solution bifurcates to a stable oscillation of period 5. The amplitude, but not the period, of these oscillations increases with further increases in D. Between $D = 45.92$ and $D = 45.93$ the periodic solution becomes unstable and the system again converges to a stable equilibrium. Further increases in D do not seem to produce additional bifurcations.

More-complex bifurcation patterns occur when males and females differ in development time as well as survival. Figure 8 shows some results for a case with $\alpha = 2$, $\beta = 3$, $P_m = 0.5$, $P_f = 0.3$. At $D = 0.1$ the population still converges to a stable equilibrium (fig. 8*a*). Figure 8 shows a phase portrait. This is a projection of the trajectory on a two-dimensional slice through the state space, plotting the proportion of adult males $(x_3 + x_4)$ against the proportion of adult females $(x_6 + x_7)$ in the population (these proportions do not sum to 1 because there are other classes in the population). The transient points shown in figure 8*b* spiral in to the equilibrium sex ratio.

Between $D = 0.1$ and $D = 0.5$ a bifurcation occurs, producing a quasi-periodic

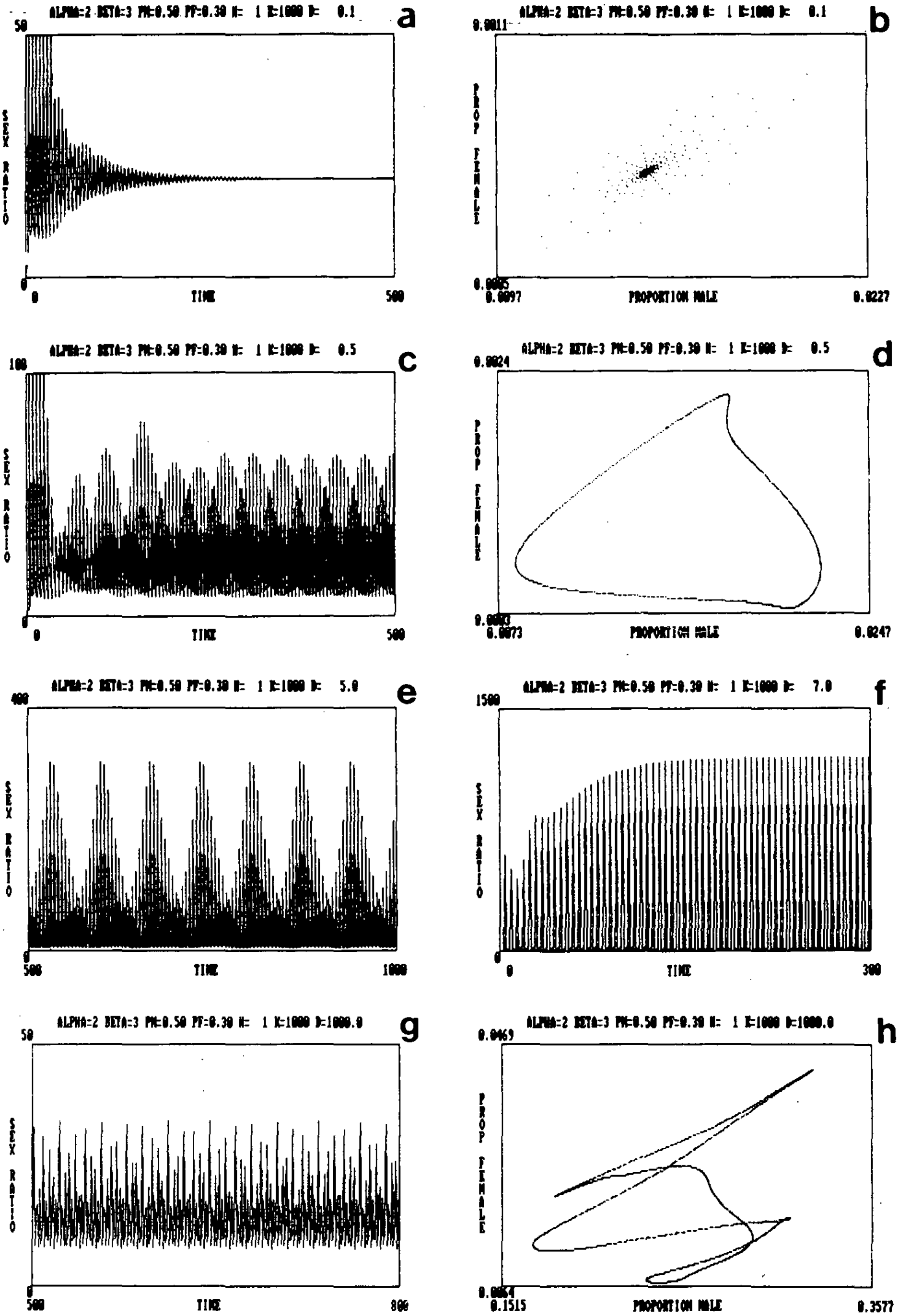

FIG. 8.—An example of bifurcation of the sex ratio as inter-stage competition (D) increases when males and females differ in both development rate and survival. *a*, $D = 0.1$; *b*, phase portrait corresponding to $D = 0.1$; *c*, $D = 0.5$; *d*, phase portrait for $D = 0.5$; *e*, $D = 5$; *f*, $D = 7$; *g*, $D = 1000$; *h*, phase portrait for $D = 1000$. (*Continued*)

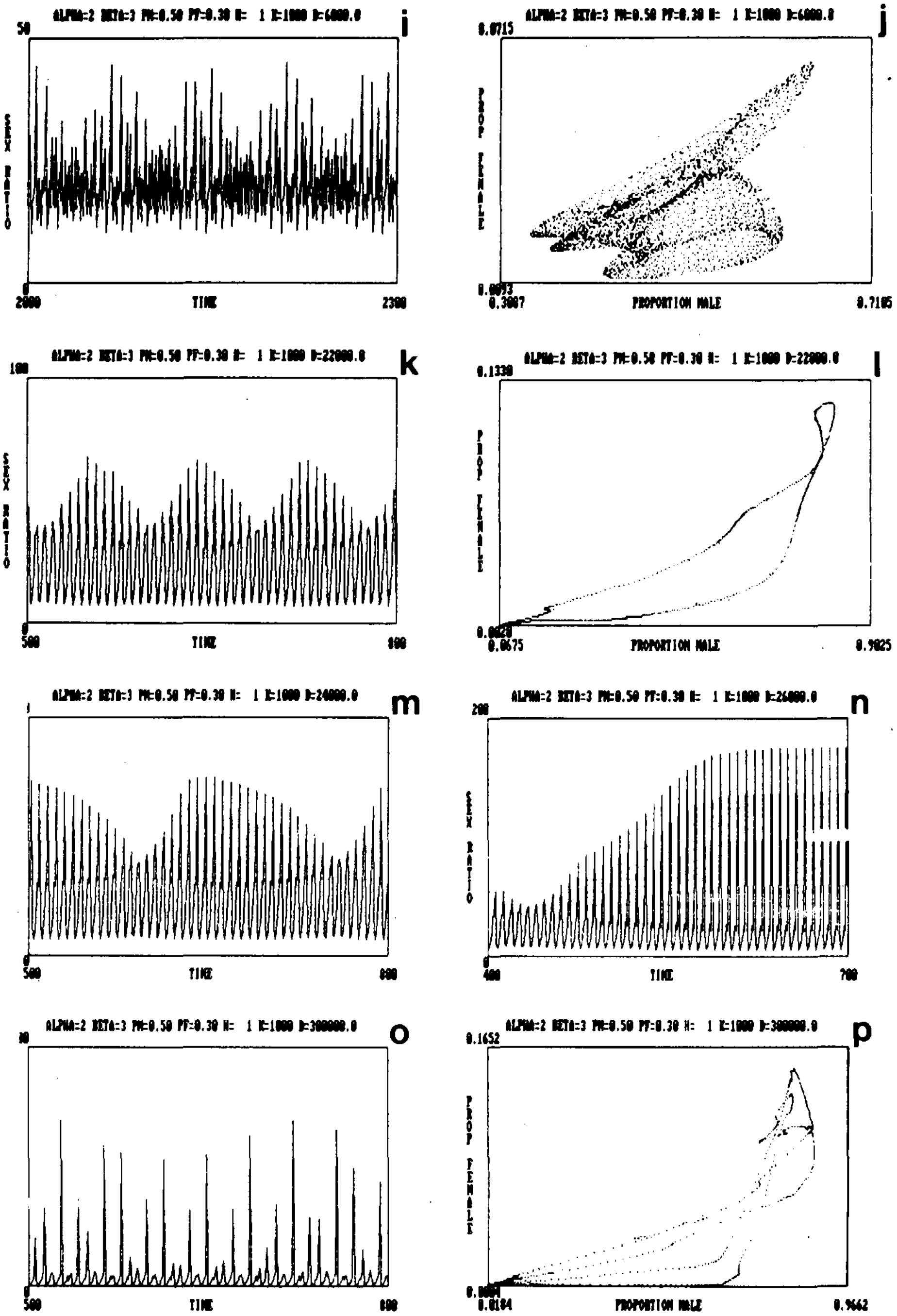

FIG. 8 (*Continued*).—*i*, D = 6000; *j*, phase portrait for D = 6000; *k*, D = 22,000; *l*, phase portrait for D = 22,000; *m*, D = 24,000; *n*, D = 26,000; *o*, D = 300,000; *p*, phase portrait for D = 300,000. Simulation details: as in figure 7, except that $\alpha = 2$, $\beta = 3$, $P_m = 0.5$, $P_f = 0.3$ throughout. $k_{46} = k_{47} = k = 1000$, and $k_{36} = k_{37} = k/100$. This simulates a situation in which experienced males are more successful at reproduction than those reproducing for the first time but there is no such difference for females.

trajectory (fig. 8*c*). The phase portrait of this trajectory (fig. 8*d*) is a continuous curve. Such quasi-periodic trajectories result from the presence of two incommensurate frequencies in the solution. As D increases, these frequencies converge, decreasing the modulation frequency (fig. 8*e*) until, between $D = 6$ and $D = 7$, "phase locking" occurs, producing a stable period-5 solution (fig. 8*f*) of large amplitude.

The amplitude of this oscillation increases between $D = 7$ and $D = 360$. Between $D = 360$ and $D = 370$ another bifurcation occurs, producing another quasi-periodic solution (fig. 8*g*) with a more complex phase portrait (fig. 8*h*), which persists until $D \approx 6000$. At this point, an apparently chaotic solution emerges (fig. 8*i*), the attractor for which is not a closed curve (fig. 8*j*). Eventually ($D = 22{,}000$, figs. 10*k*,*l*) another quasi-periodic solution emerges. Again the modulation frequency decreases (fig. 8*m*) until phase locking occurs between $D = 25{,}000$ and $D = 26{,}000$ (fig. 8*n*) and a period-7 solution appears. This periodic solution remains stable until $D \approx 300{,}000$, at which point a complex, apparently quasi-periodic solution emerges (fig. 8*o*). The phase portrait for this solution (fig. 8*p*) does not appear to be a simple closed curve; this solution may have a very high period since the gaps between the points in figure 8*p* are filled in very slowly, if at all.

We certainly do not suggest that this entire range of parameter values is biologically relevant; these results are presented to show some of the possible patterns of behavior that two-sex models with mate competition may exhibit.

This bifurcation process appears to be an example of the so-called Ruelle-Takens-Newhouse route to chaos (e.g., Eckman 1981), starting from an initial Hopf bifurcation to a quasi-periodic solution characterized by the presence of two incommensurate frequencies (very likely resulting here from the difference between male and female maturation times) and collapsing to chaos at the point where a third incommensurate frequency arises. The appearance of periodic trajectories within the quasi-periodic domain results from phase locking, which occurs when the two primary frequencies become commensurate. This bifurcation pattern is known in a variety of mathematical models (e.g., Franceschini 1983; Kaneko 1983) and experimental systems (e.g., Gollub and Benson 1980; Glass et al. 1984).

MODEL 3: AN INHOMOGENEOUS MODEL, INSTABILITY, AND EXTINCTION

Finally, we examine an interesting consequence of the sigmoid fecundity function (8). This function is not homogeneous, and theorem 1 does not apply. However, it is not without biological interest. Allen (1980) suggested that a sigmoid function might describe sperm whale pregnancy rates as a function of the availability of males. Mature female sperm whales travel in pods of about 10 individuals. Males join the pods during the breeding season and fertilize females. Female fecundity thus depends on the relative number of males and pods, and on the success of the males at finding pods at the appropriate time. May and Beddington (1980; Beddington and May 1980; May 1980) described sperm whale birth functions based on models of predator searching behavior. Although their fecundity functions are not sigmoid, such a function could easily be derived from the same assumptions leading to sigmoid functional-response curves in predator-prey models.

Numerical studies reveal that populations with sigmoid fecundity functions usually converge to a stable population structure, but that they may in some cases be driven extinct by small perturbations in the initial sex ratio. Figure 9 shows an example with $\epsilon = 3$. When clutch size $k = 10$, an initial sex ratio of 1.0 leads to a stable sex ratio, and initial sex ratios of 0.1 or 10 explode as the population collapses toward zero. (Females decline more rapidly than males in this example; otherwise, the sex ratio would collapse to zero. See fig. 9*a*.)

When clutch size is larger ($k = 20$), larger perturbations in the initial sex ratio can be tolerated. Initial sex ratios of 0.1, 1, and 10 all converge, and initial sex ratios of 0.01 or 100 diverge as the population crashes (fig. 9*b*).

To explain this pattern, we note that although equation (8) is not homogeneous of degree zero, it is asymptotically homogeneous when n_m and n_f both become large. Thus, as population size increases, the assumptions of theorem 1 become approximately true and the sex ratio eventually converges. When the population is declining, however, all bets are off; it may not even possess an equilibrium sex ratio. Since perturbations of the sex ratio affect the birth rate (e.g., fig. 2), they may trigger decreases in population size. In a homogeneous model, the sex ratio will begin to converge to the stable value and the population can begin to increase. In the sigmoid case, however, the initial decrease in population size may prevent recovery of the sex ratio and eventually lead to extinction. This effect will be most noticeable in populations that have low growth rates even at the best of times. Figure 9*c* maps out the initial sex ratios leading to growth and extinction as a function of k; at higher values of k, larger perturbations are required to trigger extinction.

CONCLUSIONS

1. The assumptions that justify one-sex demographic models are not likely to be universally met in nonhuman species. Sexual dimorphism in life history traits, skewed and fluctuating sex ratios, sex change, and the existence of multiple mating strategies may require models that include the sexes explicitly.

2. The interaction of the sexes may be described by nonlinear matrix population models. These nonlinearities are frequency-dependent; thus, the matrix elements become homogeneous functions of degree zero, and the map describing population growth is homogeneous of degree one.

3. The equilibrium population structure and reproductive value (if they exist) can be derived from the life-cycle graph by the same procedures used for linear models. If the nonlinearities affect only reproduction, equilibrium population structure reflects those nonlinearities only through the population growth rate λ. Reproductive values, however, depend in a nonlinear fashion on the equilibrium sex ratio. A general formula for the equilibrium adult sex ratio of a simple two-sex life cycle is derived.

4. In the absence of inter-stage mate competition, the equilibrium sex ratio is

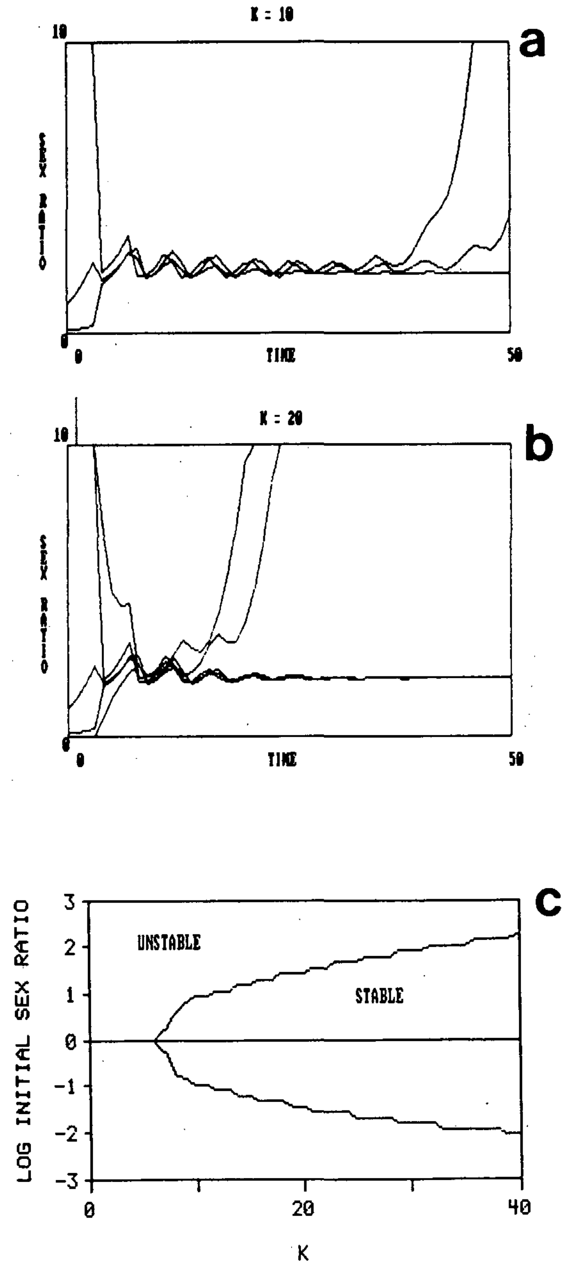

FIG. 9.—The effect of changes in the initial sex ratio on a model with the sigmoid fecundity function (eq. 8). *a*, $k = 10$, initial sex ratios of 0.1, 1, and 10. An initial sex ratio of 1.0 leads to a stable sex ratio, but initial sex ratios of 0.1 or 10 eventually diverge as the population declines to extinction. *b*, $k = 20$, initial sex ratios of 0.01, 0.1, 1, 10, and 100. All but the two extreme values converge; initial sex ratios of 0.01 or 100 lead to extinction. *c*, The initial sex ratios leading to population growth and extinction as a function of k. Simulation details: life-cycle graph as in figure 6; $\alpha = \beta = 2$, $P_m = 0.4$, $P_f = 0.3$, k_{ij} as in figure 8, $\epsilon = 3$. Male and female fecundity functions given by equation (8). Initial population size fixed at 100, with initial relative abundance of males and females in all age groups given by the initial sex ratio.

locally stable for a wide range of birth functions. If inter-stage competition is present, the equilibrium sex ratio may be unstable. Numerical studies of such models reveal bifurcations to periodic, quasi-periodic, and chaotic behaviors.

5. The rate of convergence to a stable equilibrium sex ratio depends on the extent of sexual dimorphism in life history traits, particularly age at maturity. If survival or development differs greatly between males and females, convergence is slow and accompanied by wide, transient fluctuations.

6. Sigmoid fecundity functions, which are not homogeneous, may trigger extinction as a result of fluctuations in the initial sex ratio.

7. Several important unsolved problems may be mentioned. Obviously, it is important to learn whether the parameter values leading to bifurcations, extinction, and other exotic behaviors correspond to those likely to be encountered in nature. Also, the evolutionary stability of the primary sex ratio can be analyzed using methods of evolutionarily stable strategies (ESS) and sensitivity analysis (Caswell 1978) of the population at equilibrium. However, ESS methods assume the existence of an equilibrium background against which potentially invading strategies may be evaluated. Selection on the primary sex ratio when there is no equilibrium adult sex ratio is an unsolved question (cf. Auslander et al. 1978 for corresponding problems in a density-dependent model). Density-dependent nonlinearities are also known to produce bifurcations leading eventually to chaos. It is not clear how density dependence and frequency dependence interact.

SUMMARY

Most demographic models consider only one sex, usually the female. The widespread occurrence of sexual dimorphism in life history traits and the occurrence of skewed and fluctuating sex ratios suggest that one-sex models or those dominated by one sex may often be less appropriate than two-sex models. Reproduction in two-sex models is a frequency-dependent nonlinear function (the birth or marriage function) of the relative abundance of males and females. In this paper, we examine the population dynamics resulting from three different two-sex, discrete-time, population-projection models. For a large class of birth functions, models without inter-stage mate competition are shown to converge to a locally stable adult sex ratio. Formulas for the stable population structure, stable sex ratio, and reproductive value at equilibrium are derived. When individuals of different stages compete for mates, the equilibrium population structure may become unstable. A sequence of bifurcations then occurs, leading to periodic oscillations, quasi-periodic fluctuations, and chaos as the intensity of competition increases. Finally, when per capita fecundity is a sigmoid function of the relative abundance of the other sex, perturbations of the sex ratio may lead to extinction.

ACKNOWLEDGMENTS

We thank J. Cohen, R. Lee, R. Nussbaum, V. Protopopescu, S. Tuljapurkar, K. Wachter, and three anonymous referees for helpful discussions and comments on an earlier version of this manuscript. This research was supported by National

Science Foundation grant BSR 82-14583, by National Oceanic and Atmospheric Administration National Sea Grant College Program grant NA80-AA-D-00077 (H.C.), and by a Woods Hole Oceanographic Institution Summer Student Fellowship (D.W.). Woods Hole Oceanographic Institution contribution 5933.

APPENDIX A

THEOREM I

Proof

We assume the existence of an equilibrium vector **w**, and ask whether initial populations not proportional to **w** will converge to it. Since the equilibrium population is not a constant solution of the equations (1), we cannot directly apply the usual local-stability analysis (e.g., Beddington 1974) for equilibrium points of discrete nonlinear systems. Instead, we generalize this analysis to focus on convergence of population structure, not absolute abundance.

Choose a reference solution $\mathbf{n}_s(t)$ to the nonlinear map

$$\mathbf{n}(t + 1) = \pi[\mathbf{n}(t)], \tag{A1}$$

and consider the nature of solutions that start near $\mathbf{n}_s$. (We are interested in reference solutions along which population structure is at equilibrium, so that $\mathbf{n}_s$ will be proportional to **w**.) Define the deviation $\mathbf{y}(t) = \mathbf{n}(t) - \mathbf{n}_s(t)$. The dynamics of this deviation are given by

$$\begin{aligned} \mathbf{y}(t + 1) &= \mathbf{n}(t + 1) - \mathbf{n}_s(t + 1) \\ &= \pi[\mathbf{y}(t) + \mathbf{n}_s(t)] - \pi[\mathbf{n}_s(t)]. \end{aligned} \tag{A2}$$

Expanding $\pi(\ )$ in a Taylor series about $\mathbf{n}_s$ and neglecting second-order terms gives a linear approximation for **y**:

$$\mathbf{y}(t + 1) = \left(\frac{\partial \pi}{\partial \mathbf{n}}\right)\mathbf{y}(t), \tag{A3}$$

where the matrix of partial derivatives is evaluated along the reference solution $\mathbf{n}_s$.

In our case, the *i*th component of π is

$$\pi_i = \sum_k a_{ik} n_k; \tag{A4}$$

thus, $\partial \pi_i/\partial n_j = a_{ij} + \Sigma_k n_k \partial a_{ik}/\partial n_j$, with both a_{ij} and the latter partial derivative being evaluated along $\mathbf{n}_s(t)$.

The resulting approximation for the deviation from the reference solution is

$$\mathbf{y}(t + 1) = [\mathbf{A}(t) + \mathbf{Q}(t)]\mathbf{y}(t) = \mathbf{B}(t)\mathbf{y}(t), \tag{A5}$$

where

$$q_{ij} = \sum_k n_k \frac{\partial a_{ik}}{\partial n_j}. \tag{A6}$$

If $\mathbf{y}(t)$ goes to zero, then the solution $\mathbf{n}(t)$ certainly converges to the reference solution. However, this convergence is stronger than necessary for the convergence of population structure, which requires only that $\mathbf{n}(t)$ become proportional to $\mathbf{n}_s(t)$. An appropriate measure of the difference between the two solutions is thus Hilbert's projective metric (Golubitsky et al. 1975). This metric measures the distance $d(\mathbf{a}, \mathbf{b})$ between two nonnegative vectors **a** and **b** in such a way that $d = 0$ whenever $\mathbf{a} = c\mathbf{b}$ for any $c > 0$, and it can be written

$$d(\mathbf{a}, \mathbf{b}) = \ln\,[\max_i(a_i/b_i)]/[\min_i(a_i/b_i)]. \tag{A7}$$

We will rely on a theorem of Birkhoff (1957; see Golubitsky et al. 1975; Seneta 1981, chap. 3), which states that multiplication by any positive (or nonnegative and primitive) matrix $\mathbf{D}$ is a strict contraction in terms of the projective metric. That is, $d(\mathbf{Dx}, \mathbf{Dy}) < d(\mathbf{x}, \mathbf{y})$ for any positive $\mathbf{x}$ and $\mathbf{y}$.

When $\mathbf{n}(t)$ is proportional to $\mathbf{n}_s(t)$, $d[\mathbf{y}(t), \mathbf{n}_s(t)] = 0$; thus, our proof of stability will apply Birkhoff's theorem to the projective distance between $\mathbf{y}$ and $\mathbf{n}_s$. We assume that $\mathbf{y}(0)$ is positive (so that the projective metric can be calculated). We can always modify $\mathbf{n}_s(0)$ to make it positive because the magnitude of the initial population along the reference vector $\mathbf{w}$ is arbitrary.

The applicability of Birkhoff's theorem depends on the nature of $\mathbf{B}(t)$ in equation (12). Since $\mathbf{A}$ is homogeneous of degree zero, it is constant along the reference solution. Since the derivative of a homogeneous function of degree zero is homogeneous of degree -1, the products $n_k \partial a_{ik}/\partial n_j$, which make up the elements of $\mathbf{Q}$, are also constant along $\mathbf{n}_s$. Thus, $\mathbf{B} = \mathbf{A} + \mathbf{Q}$ is constant.

Consider $\mathbf{Bw} = \mathbf{Aw} + \mathbf{Qw}$. We know that $\mathbf{Aw} = \lambda\mathbf{w}$. Let $\mathbf{Qw} = \mathbf{g}$. Then

$$g_i = \sum_h \sum_k n_k w_h \left(\frac{\partial a_{ik}}{\partial n_h}\right). \tag{A8}$$

Since $\mathbf{n}_s$ is proportional to $\mathbf{w}$, g_i is proportional to

$$\sum_k n_k \sum_h n_h \left(\frac{\partial a_{ik}}{\partial n_h}\right), \tag{A9}$$

which, by Euler's theorem on homogeneous functions, equals zero. Thus $\mathbf{Bw} = \mathbf{Aw} + 0$, and both the deviation vector $\mathbf{y}$ and the reference solution vector $\mathbf{n}_s$ are being multiplied by the same matrix.

Since $\mathbf{y}(t)$ and $\mathbf{n}_s(t)$ are both multiplied by the same matrix $\mathbf{B}$, Birkhoff's theorem guarantees that the projective distance $d[\mathbf{y}(t), \mathbf{n}_s(t)]$ between them is strictly decreasing if $\mathbf{B}$ is nonnegative and primitive.

$\mathbf{A}$ is nonnegative and assumed to be primitive. Since $b_{ij} = a_{ij} + q_{ij}$, a sufficient (but stronger than necessary) condition for nonnegativity and primitivity of $\mathbf{B}$ is that $a_{ij} + q_{ij} > 0$.

Write q_{ij} as

$$q_{ij} = n_j \frac{\partial a_{ij}}{\partial n_j} + \sum_{k \neq j} n_k \frac{\partial a_{ik}}{\partial n_j}. \tag{A10}$$

The first term of equation (A10) can be evaluated using equation (15), yielding

$$q_{ij} = k_{ij} \frac{\partial M_{ij}(X_{ij})}{\partial n_j} - a_{ij} + \sum_{k \neq j} n_k \frac{\partial a_{ik}}{\partial n_j}. \tag{A11}$$

Since the derivative of a mean with respect to any of its terms is positive, the summation in equation (A10) is nonnegative and is strictly positive if n_j is included in at least one of the sets X_{ik}. Thus $a_{ij} + q_{ij}$ is clearly nonnegative and is strictly positive if n_j appears in at least one of the sets X_{ik}. Our earlier assumption that $n_j \in X_{ij}$ suffices to guarantee that $a_{ij} + q_{ij}$ is strictly positive. This completes the proof.

Notes

1. Theorem 1 gives sufficient conditions for convergence; they are not necessary. For example, if n_j is not an element of X_{ik} for any k, then $b_{ij} = 0$. This causes problems for the theorem only because it may render $\mathbf{B}$ imprimitive. But if it does not do so (and this may be evaluated in specific cases by inspection of the life-cycle graph), the theorem still holds.

2. Theorem 1 extends immediately to cases in which a_{ij} is a positive linear combination of means, with possibly different weights and values of r, and possibly including different subsets of the n_i. In this case, q_{ij} becomes a sum of terms, each of which is given by equation (A10), and the nonnegativity results apply to each term individually.

3. Although it is of less biological interest, a similar calculation shows that if $a_{ij} = k_{ij}M_{ij}/n_i$ (i.e., the transition from stage j to stage i is limited by competition within stage i rather than stage j), then q_{ij} is always nonnegative, and stability is always guaranteed.

APPENDIX B

Competition and Instability

We demonstrate here that the stability proof of Appendix A does not apply to a matrix **A** defined by equation (19) and otherwise satisfying the assumptions of theorem 1.

We assume that

$$a_{ij} = [\Sigma_h M_{ijh}(X_{ijh})]/(n_j + C_{ij}), \tag{B1}$$

where the index h ranges over some set H_{ij}, which may differ for each a_{ij}.

To evaluate equation (A10) for q_{ij}, we need expressions for $\partial a_{ik}/\partial n_j$, for all k. To avoid a bothersome proliferation of summations and subscripts, assume for the moment that H_{ik} contains only one element. Then, writing M'_{ij} for $\partial M_{ij}/\partial n_j$ and C'_{ij} for $\partial C_{ij}/\partial n_j$, we have

$$\frac{\partial a_{ij}}{\partial n_j} = \frac{(n_j + C_{ij})M'_{ij} - M_{ij}(1 + C'_{ij})}{(n_j + C_{ij})^2}, \tag{B2}$$

and, for $k \neq j$,

$$\frac{\partial a_{ik}}{\partial n_j} = \frac{(n_k + C_{ik})M'_{ik} - M_{ik}C'_{ik}}{(n_k + C_{ik})^2}. \tag{B3}$$

Substituting equations (B2) and (B3) into equation (A10) yields an expression for q_{ij}:

$$q_{ij} = \left[\frac{M'_{ij}}{n_j + C_{ij}} - \frac{M_{ij}}{(n_j + C_{ij})^2}\right] n_j + \sum_k \left[\frac{M'_{ik}}{n_k + C_{ik}}\right] n_k - \sum_k \left[\frac{M_{ik}C'_{ik}}{(n_k + C_{ik})^2}\right] n_k. \tag{B4}$$

When H_{ij} contains more than one index, so that equation (B1) really is a sum of terms, q_{ij} is a sum of terms of the form (B4). From equation (B4) it is obvious that $b_{ij} = q_{ij} + a_{ij}$ may be negative, especially when $C'_{ik} \gg 0$ for some k, that is, when inter-stage competition is intense. If $b_{ij} < 0$, Birkhoff's theorem no longer applies and the population structure is no longer guaranteed to converge to **w**.

LITERATURE CITED

Adams, J., P. Greenwood, and I. Swingland. 1985. Sex in an unpredictable world. New Sci. 105(1442):32–34.

Allen, K. R. 1980. Conservation and management of whales. University of Washington Press, Seattle.

Alstad, D. N., and G. F. Edmunds, Jr. 1983. Selection, outbreeding depression, and the sex ratio of scale insects. Science (Wash., D.C.) 220:93–95.

Altman, P. L., and D. S. Dittmer. 1962. Growth, including reproduction and morphological development. Biological Handbooks, Federation of American Societies for Experimental Biology, Washington, D.C.

Auslander, D., J. Guckenheimer, and G. Oster. 1978. Random evolutionarily stable strategies. Theor. Popul. Biol. 13:276–293.

Beddington, J. 1974. Age distribution and the stability of simple discrete time population models. J. Theor. Biol. 47:65–74.

Beddington, J. R., and R. M. May. 1980. A possible model for the effect of adult sex ratio and density on the fecundity of sperm whales. Rep. Int. Whal. Comm. Spec. Issue 2:73–74.

Bell, G. 1982. The costs of reproduction and their consequences. Am. Nat. 116:45–76.

Birkhoff, G. 1957. Extensions of Jentzch's theorem. Trans. Am. Math. Soc. 85:219–227.

Caswell, H. 1978. A general formula for the sensitivity of population growth rate to changes in life history parameters. Theor. Popul. Biol. 14:215–230.

———. 1982. Stable population structure and reproductive value for populations with complex life cycles. Ecology 63:1223–1231.

Caswell, H., R. J. Naiman, and R. Morin. 1984. Evaluating the consequences of reproduction in complex salmonid life cycles. Aquaculture 343:123–134.

Cavalli-Sforza, L. L., and W. F. Bodmer. 1971. The genetics of human populations. Freeman, San Francisco.

Charnov, E. L. 1982. The theory of sex allocation. Princeton University Press, Princeton, N.J.

Clutton-Brock, T. H., F. E. Guinness, and S. D. Albon. 1982. Red deer: behavior and ecology of two sexes. University of Chicago Press, Chicago.

Clutton-Brock, T. H., S. D. Albon, and F. E. Guinness. 1985. Parental investment and sex differences in juvenile mortality in birds and mammals. Nature (Lond.) 313:131–133.

Comfort, A. 1979. The biology of senescence. 3d ed. Elsevier, New York.

Corkett, C. J., and I. A. McLaren. 1978. The biology of *Pseudocalanus*. Adv. Mar. Biol. 15:1–231.

Darwin, C. 1871. The descent of man and selection in relation to sex. John Murray, London.

Das Gupta, P. 1972. On two-sex models leading to stable populations. Theor. Popul. Biol. 3:358–375.

———. 1978. An alternative formulation of the birth function in a two-sex model. Popul. Stud. 32: 367–379.

Deevey, G. B., and E. S. Deevey, Jr. 1945. A life table for the black widow. Trans. Conn. Acad. Arts Sci. 36:115–134.

Dingle, H. 1966. The effect of population density on mortality and sex ratio in the milkweed bug, *Oncopeltus*, and the cotton stainer, *Dysdercus* (Heteroptera). Am. Nat. 100:465–470.

Eckman, J.-P. 1981. Roads to turbulence in dissipative dynamical systems. Rev. Mod. Phys. 53: 643–654.

The Economist. 1985. Alas, for women of a certain age. January 12, 26–27.

Ehrlich, P. R., A. E. Launer, and D. D. Murphy. 1984. Can sex ratio be defined or determined? The case of a population of checkerspot butterflies. Am. Nat. 124:527–539.

Fisher, R. A. 1958. The genetical theory of natural selection. 2d ed. Dover, New York.

Franceschini, V. 1983. Bifurcations of tori and phase locking in a dissipative system of differential equations. Physica 6D:285–304.

Frederickson, A. G. 1971. A mathematical theory of age structure in sexual populations: random mating and monogamous marriage models. Math. Biosci. 10:117–143.

Geiser, S. W. 1924. The differential death-rate of the sexes among animals. Wash. Univ. Stud. 12:73.

Gibbons, J. W., R. D. Semlitsch, J. L. Greene, and J. P. Schubauer. 1981. Variation in age and size at maturity of the slider turtle (*Pseudemys scripta*). Am. Nat. 117:841–845.

Glass, L., M. R. Guevara, J. Belair, and A. Shrier. 1984. Global bifurcations of a periodically forced biological oscillator. Phys. Rev. A29:1348–1357.

Goldman, N., C. F. Westoff, and C. Hammerslough. 1984. Demography of the marriage market in the United States. Popul. Index 50:5–25.

Gollub, J. P., and S. V. Benson. 1980. Many routes to turbulent convection. J. Fluid Mech. 100: 449–470.

Golubitsky, M., E. B. Keeler, and M. Rothschild. 1975. Convergence of the age structure: applications of the projective metric. Theor. Popul. Biol. 7:84–93.

Gould, S. J. 1983. Hen's teeth and horse's toes. Norton, New York.

Gross, M. R. 1984. Sunfish, salmon, and the evolution of alternative reproductive strategies and tactics in fishes. Pages 55–76 *in* G. W. Potts and R. J. Wootton, eds. Fish reproduction: strategies and tactics. Academic Press, New York.

Guckenheimer, J., G. Oster, and A. Ipaktchi. 1977. The dynamics of density dependent population models. J. Math. Biol. 4:101–147.

Hamilton, W. D. 1967. Extraordinary sex ratios. Science (Wash., D.C.) 156:477–488.

Hardy, G. H., J. E. Littlewood, and G. Polya. 1952. Inequalities. 2d ed. Cambridge University Press, Cambridge.

Holden, C. 1983. Can smoking explain ultimate gender gap? Science (Wash., D.C.) 221:1034.

Hubbell, S. P., and P. A. Werner. 1979. On measuring the intrinsic rate of increase of populations with heterogeneous life histories. Am. Nat. 113:277–293.

Jones, J. W. 1959. The salmon. Harper & Bros., New York.

Kaneko, K. 1983. Transition from torus to chaos accompanied by frequency lockings with symmetry breaking. Prog. Theor. Phys. 69:1427–1442.

Keyfitz, N. 1968. Introduction to the mathematics of population. Addison-Wesley, Reading, Mass.

———. 1972. The mathematics of sex and marriage. Proc. 6th Berkeley Symp. Math. Stat. Prob. 4: 89–108.

Keyfitz, N., and W. Flieger. 1971. Population: facts and methods of demography. Freeman, San Francisco.

Levin, S. A., and C. P. Goodyear. 1980. Analysis of an age-structured fishery model. J. Math. Biol. 9:245–274.

Luppova, E. P., and E. Y. Frisman. 1983. Stationarity and stability of a dynamical system describing the behavior of a dioecious population. Pages 84–92 *in* Differential and operator equations in function spaces. USSR Academy of Sciences, Far East Science Center, Vladivostok.

MacArthur, J. W., and W. H. T. Baillie. 1932. Sex differences in mortality in *Abraxas*-type species. Q. Rev. Biol. 7:313–325.

Maly, E. J. 1970. The influence of predation on the adult sex ratios of two copepod species. Limnol. Oceanogr. 15:566–573.

Marshall, S. M., and A. P. Orr. 1955. The biology of a marine copepod, *Calanus finmarchicus* (Gunnerus). Oliver & Boyd, Edinburgh.

Maufette, Y., and L. Jobin. 1985. Effects of density on the proportion of male and female pupae in gypsy-moth populations. Can. Entomol. 117:535–539.

May, R. M. 1980. Mathematical models in whaling and fisheries management. Lect. Math. Life Sci. 13:1–64.

May, R. M., and J. R. Beddington. 1980. The effect of adult sex ratio and density on the fecundity of sperm whales. Rep. Int. Whal. Comm. Spec. Issue 2:213–217.

McFarland, D. D. 1972. Comparison of alternative marriage models. Pages 89–106 *in* T. N. E. Greville, ed. Population dynamics. Academic Press, New York.

Meagher, T. R. 1981. Population biology of *Chamaelirium luteum*, a dioecious lily. II. Mechanisms governing sex ratios. Evolution 35:557–567.

———. 1982. The population biology of *Chamaelirium luteum*, a dioecious member of the lily family: two-sex population projections and stable population structure. Ecology 63:1701–1711.

Meagher, T. R., and J. Antonovics. 1982*a*. The population biology of *Chamaelirium luteum*, a dioecious member of the lily family: life history studies. Ecology 63:1690–1700.

———. 1982*b*. Life history variation in dioecious plant populations: a case study of *Chamaelirium luteum*. Pages 139–154 *in* H. Dingle and J. P. Hegmann, eds. Evolution and genetics of life histories. Springer-Verlag, New York.

Mitra, S. 1978. On the derivation of a two-sex stable population model. Demography 15:541–548.

Nevo, E. 1979. Adaptive convergence and divergence of subterranean mammals. Annu. Rev. Ecol. Syst. 10:269–308.

Nussbaum, R. D. 1986. Convexity and log convexity for the spectral radius. Linear Algebra Appl. 73:59–122.

Parlett, B. 1972. Can there be a marriage function? Pages 107–135 *in* T. N. E. Greville, ed. Population dynamics. Academic Press, New York.

Pearl, R. 1928. The rate of living. Knopf, New York.

Policansky, D. 1982. Sex change in plants and animals. Annu. Rev. Ecol. Syst. 13:471–495.

Pollak, R. A. 1986. A reformulation of the two-sex problem. Demography (in press).

Pollard, J. H. 1973. Mathematical models for the growth of human populations. Cambridge University Press, Cambridge.

———. 1977. The continuing attempt to incorporate both sexes into marriage analysis. Pages 291–309 *in* 18th Int. Popul. Conf., Mexico, 1977. International Union for the Scientific Study of Population, Liège, Belgium.

Raper, J. R. 1966. Life cycles, basic patterns of sexuality, and sexual mechanisms. Pages 473–512 *in* G. C. Ainsworth and A. A. Sussman, eds. The fungi: an advanced treatise. Vol. 2. Academic Press, New York.

Robinson, A. S. 1983. Sex-ratio manipulation in relation to insect pest control. Annu. Rev. Genet. 17:191–214.

Rosen, K. H. 1983. Mathematical models for polygamous mating systems. Math. Model. 4:27–39.

Samuelson, P. A. 1976. Time symmetry and asymmetry in population and deterministic dynamic systems. Theor. Popul. Biol. 9:82–122.

Schoen, R. 1981. The harmonic mean as the basis of a realistic two-sex marriage model. Demography 18:201–216.

———. 1983. Measuring the tightness of a marriage squeeze. Demography 20:61–78.

———. 1984. Relationships in a simple harmonic mean two-sex fertility model. J. Math. Biol. 18: 201–211.

Seneta, E. 1981. Non-negative matrices and Markov chains. 2d ed. Springer-Verlag, New York.

Sherman, P. W., and M. L. Morton. 1984. Demography of Belding's ground squirrels. Ecology 65:1617–1628.

Tande, K. S., and S. Gronvik. 1983. Ecological investigations on the zooplankton community of Balsfjorden, northern Norway: sex ratio and gonad maturation cycle in the copepod *Metridia longa* (Lubbock). J. Exp. Mar. Biol. Ecol. 71:43–54.

Trivers, R. 1985. Social evolution. Benjamin/Cummings, Menlo Park, Calif.

Wade, M. J. 1984. Variance-effective population number: the effects of sex ratio and density on the mean and variance of offspring numbers in the flour beetle, *Tribolium castaneum*. Genet. Res. 43:249–256.

Willson, M. F. 1983. Plant reproductive ecology. Wiley, New York.

Willson, M. F., and N. Burley. 1983. Mate choice in plants. Princeton University Press, Princeton, N.J.

Wingard, D. L. 1984. The sex differential in morbidity, mortality, and lifestyle. Annu. Rev. Public Health 5:433–458.

Yellin, J., and P. A. Samuelson. 1974. A dynamical model for human population. Proc. Natl. Acad. Sci. USA 71:2813–2817.

———. 1977. Comparison of linear and nonlinear models for human population dynamics. Theor. Popul. Biol. 11:105–126.